Characterization of the Rab8-specific membrane traffic route linked to protrusion formation

Katarina Hattula[1], Johanna Furuhjelm[1], Jaana Tikkanen[1], Kimmo Tanhuanpää[1], Pirjo Laakkonen[2] and Johan Peränen[1,*]

[1]Institute of Biotechnology, PO Box 56 (Viikinkaari 9), FIN-00014 University of Helsinki, Finland
[2]Molecular Cancer Biology Research Program, Biomedicum Helsinki, P.O. Box 63 (Haartmaninkatu 8), FIN-00014 University of Helsinki, Finland
*Author for correspondence (e-mail: johan.peranen@helsinki.fi)

Accepted 22 September 2006
Journal of Cell Science 119, 4866-4877 Published by The Company of Biologists 2006
doi:10.1242/jcs.03275

Summary

Rab8 has a drastic effect on cell shape, but the membrane trafficking route it regulates is poorly defined. Here, we show that endogenous and ectopically expressed Rab8 is associated with macropinosomes generated at ruffling membrane domains. These macropinosomes fuse or transform into tubules that move toward the cell center, from where they are recycled back to the leading edge. The biogenesis of these tubules is dependent on actin and microtubular dynamics. Expression of dominant-negative Rab8 mutants or depletion of Rab8 by RNA interference inhibit protrusion formation, but promote cell-cell adhesion and actin stress fiber formation, whereas expression of the constitutively active Rab8-Q67L has the opposite effect. Rab8 localization overlaps with both Rab11 and Arf6, and is functionally linked to Arf6. We also demonstrate that Rab8 activity is needed for the transport of transferrin and the transferrin receptor to the pericentriolar region and to cell protrusions, and that Rab8 controls the traffic of cholera toxin B to the Golgi compartment. Finally, Rab8 colocalizes and binds specifically to a synaptotagmin-like protein (Slp1/JFC1), which is involved in controlling Rab8 membrane dynamics. We propose that Rab8 regulates a membrane-recycling pathway that mediates protrusion formation.

Supplementary material available online at
http://jcs.biologists.org/cgi/content/full/119/23/4866/DC1

Key words: GTPase, Rab8, Arf6, Membrane recycling, Protrusion

Introduction

Cell migration is crucial for processes such as embryonic development, metastasis, wound healing and inflammation. During migration, cells polarize and acquire a leading edge and a tracking tail (Lauffenburger and Horwitz, 1996). The leading edge has actin-containing filopodia and lamellipodia that participate in the forward movement (Mitchison and Cramer, 1996), which is driven by the formation of new cell-substrate contacts in the leading edge and the dissociation of cell-substrate contacts in the tracking tail (Laukaitis at al., 2001). It is unknown how the cell coordinates protrusion, traction and detachment, but regulators of these processes include small GTPases of the Rho family (Nobes and Hall, 1999).

The role of membrane vesicle transport in modulation of cell shape is controversial (Heat and Holifield, 1991). It has been suggested that membrane internalized by coated pits is returned to the plasma membrane at the leading edge, where it helps to extend the cell forward (Bretscher, 1996). Whether this membrane flow operates separately from actin dynamics is not yet clear. However, recent studies indicate that an Arf6 modulates cell morphogenesis and motility by modulating actin dynamics and the turnover of adhesion receptors (Palacios et al., 2001; Powelka et al., 2004). Arf6 regulates a clathrin-independent endocytic pathway, through which molecules like the major histocompability complex class I protein (MHCI), CD59 and the interleukin-2 receptor α subunit (Tac) are internalized (Naslavsky et al., 2004). Moreover, Arf6 also participate in processes like exocytosis, phagocytosis and cytokinesis (D'Souza-Schorey and Chavrier, 2006).

Rab GTPases regulate various membrane transport pathways, and each Rab protein has a distinct location corresponding to the pathway that it regulates (Zerial and McBride, 2001). We have shown that Rab8 promotes the polarized transport of newly synthesized membrane proteins in fibroblasts (Peränen et al., 1996), but Rab8 has only a minor effect on the transport kinetics of these membrane proteins (Ang et al., 2003; Peränen et al., 1996). Instead, ectopically expressed Rab8 has a great impact on the cell shape (Armstrong et al., 1996; Peränen et al., 1996), and cell morphogenesis is affected by a Rab8-specific GDP/GTP exchange factor and the Rab8-interacting protein optineurin (FIP-2) (Hattula and Peränen, 2000; Hattula et al., 2002; Rezaie et al., 2002). Furthermore, a mutant Rab8 causes apoptosis of transgenic *Xenopus* rods, and depletion of Rab8 from neurons inhibits neurite outgrowth (Huber et al., 1995; Moritz et al., 2001).

Here we have investigated the compartmentalization of Rab8 and its role in regulating cell morphogenesis. By observing Rab8 in living cells we found that it is associated with macropinosomes that transform into Rab8-specific tubular structures that move toward the cell center. A rapid Rab8-dependent recycling of these membranes back to the plasma membrane participates in the formation of new cell surface protrusions. The Rab8-specific membrane transport route

contained several markers known to undergo internalization and recycling (β1 integrin, transferrin, transferrin receptor, MHCI), or to participate in membrane recycling or secretion (Arf6, JFC1, Rab11).

Results

Knockdown of Rab8 affects cell morphogenesis

Overexpression of wild-type or constitutively active Rab8 (Q67L) results in the formation of cell protrusion, but the effect of the dominant-negative mutant on cell morphogenesis and membrane transport is unknown (Peränen et al., 1996). To understand better the role of Rab8 in mediating cell shape changes we stably transfected HT1080 fibrosarcoma cells with a dominant-negative (T22N) Rab8, a constitutively active (Q67L) Rab8 or their N-terminal green fluorescent protein (GFP) fusions (Fig. 1D). Vector-only (pIRES-neo or pEGFP-C1) cells formed loose, semi-ordered contacts with each other (Fig. 1A) while cells expressing dominant-negative Rab8-T22N were cuboidal, and formed close cell-cell contacts (Fig. 1C). Cells expressing constitutively active Rab8-Q67L were spindle shaped, lost contact inhibition and grew on top of each other (Fig. 1B).

To determine if endogenous Rab8 plays a role in cell morphogenesis, HT1080 cells were transiently transfected with small interfering RNAs (siRNA) directed against a control sequence (Bertling et al., 2004) or against the Rab8 sequence (Schuck et al., 2004). Cell transfected with the Rab8-specific siRNA showed a clear decrease in Rab8 protein content (80-90%) when compared with the control siRNA (Fig. 1K). Cells treated with the control siRNA for 2 days grew in an unordered fashion, independently of cell density, and they were asymmetric (Fig. 1E,G). By contrast, cells depleted of Rab8 made close cell-cell contacts, and had a symmetrical morphology (Fig. 1F,H). We noted that cells depleted of Rab8 were devoid of lamellipodia-like structures, but obtained strong actin stress fibers in the middle of the cell (Fig. 1J). Cells transfected with the control siRNA showed lamellipodia-like structures typical for HT1080 cells, and were devoid of actin stress fibers (Fig. 1I). Taken together, our results show that Rab8 is essential for the maintenance of the normal HT1080 cell phenotype: asymmetric shape, protrusive activity and loss of contact inhibition.

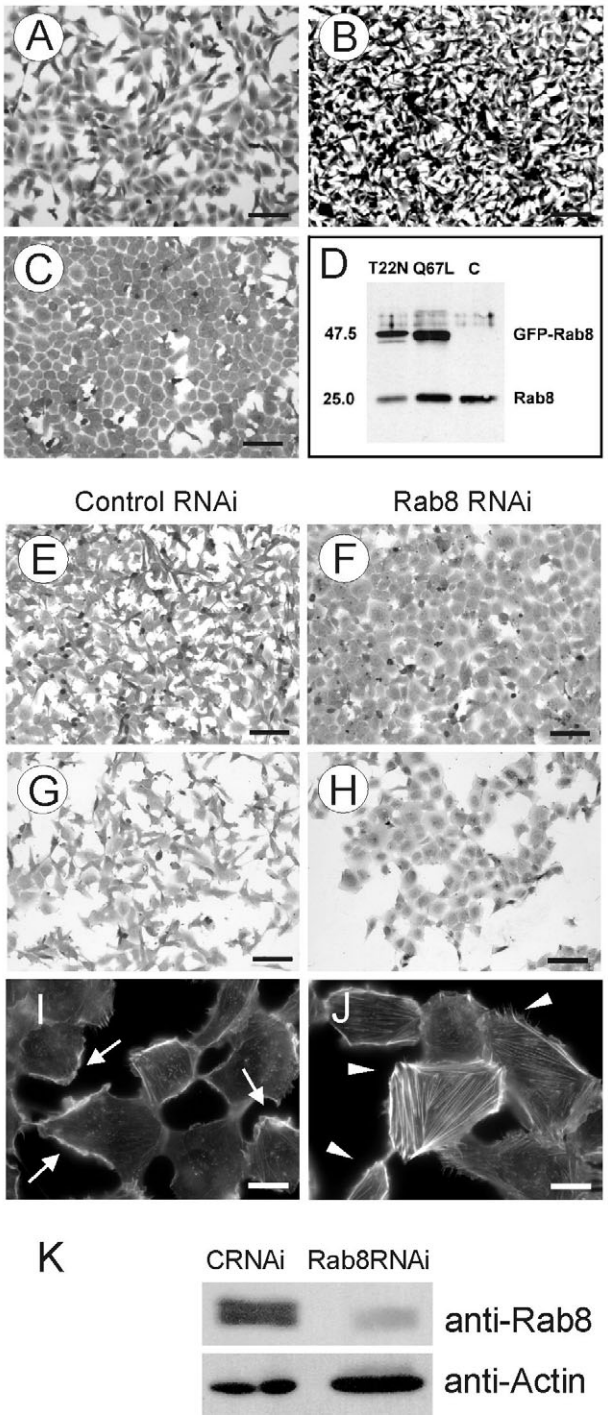

Role of Rab8 in polarized transferrin recycling and cholera toxin trafficking

Rab proteins are known to control receptor-mediated endocytosis and recycling (Zerial and McBride, 2001). To test whether Rab8 is linked to these pathways we studied the colocalization of endogenous Rab8 with different Rab proteins expressed as GFP-fusions. There was no colocalization of endogenous Rab8 with GFP-Rab4 and GFP-Rab5 in HT1080 cells (Fig. 2A,B). Rab5-positive vesicles were concentrated in a region behind the leading edge, whereas Rab8-positive vesicles and macropinosomes were found in the outmost region of the leading edge (Fig. 2B). GFP-Rab11 partially colocalized with endogenous Rab8 on small vesicles (Fig. 2). However,

Fig. 1. Rab8 modulates cell shape changes. (A) A control stable cell line expressing GFP (green fluorescent protein) form semi-ordered contacts, while (B) a stable cell line expressing Rab8-Q67L (pEGFP-Rab8-Q67L) have lost contact inhibition and (C) a stable cell line expressing Rab8-T22N (pEGFP-Rab8-T22N) shows close cell-cell contacts. (D) Expression of EGFP-Rab8-T22N, EGFP-RabQ67L (GFP-Rab8) and endogenous Rab8 (Rab8) in these stable cell lines was monitored by western blotting. (E-K) Depletion of Rab8 from HT1080 fibrosarcoma cells by RNAi. HT1080 cells were transfected with control RNAi (E,G,I) or with Rab8-specific RNAi (F,H,J). Note that Rab8 depletion promotes cell-cell adhesion (F,H). Arrows indicated cells with lamellar structures (I), whereas cells containing actin stress fibers are indicated by arrowheads (J). (K) Total lysates from cells transfected with control or Rab8-specific RNAi were analyzed by western blotting by anti-actin and anti-Rab8 antibodies. Bars, 200 μM (A-C,E-H), 20 μM (I,J).

Rab11 was not detected on Rab8-specific tubules (data not shown). Ectopically expressed myc-Rab8-Q67L also showed overlap with GFP-Rab11 (Fig. 2J-L), though unlike Rab11 Rab8 was more frequently associated with the plasma membrane and ruffles.

Partial colocalization of Rab8 with Rab11 suggests that Rab8 might affect the trafficking of transferrin (Tfn) and the transferrin receptor (Tfn-R). Thus, we studied the effect of Rab8 depletion on Tfn internalization and recycling. Initially, we confirmed by immunofluorescence microscopy and by western blotting that Rab8 can be depleted from HeLa cells by Rab8-specific siRNA (Fig. 3). Then HeLa cells, transfected with the control siRNA or the Rab8-specific siRNA, were pulsed (30 minutes) with Alexa-labeled Tfn and then chased (30 minutes) in the presence of serum. After the pulse Tfn had reach the pericentriolar region of the control cells, but in Rab8-depleted cells Tfn was found in small vesicles scattered randomly in the cytoplasm (Fig. 3). Even a longer pulse (60 minutes) did not lead to accumulation of Tfn in the pericentriolar region of Rab8-depleted cells (not shown). After the chase period most of the Tfn was externalized both from the control cells and the Rab8-depleted cells (Fig. 3E-H). Thus, Rab8 is not essential for the internalization and recycling of Tfn, but it is needed for delivery to the pericentriolar region. Next we looked at the distribution of Tfn-R in Rab8-depleted cells (supplementary material Fig. S1). In control HeLa cells about 60% of the cells had TFn-R accumulated in the pericentriolar region, and in 30% of the cells Tfn-R colocalized with Rab8 in protrusions (supplementary material Fig. S1A-D). By contrast, the Tfn-R was randomly located in small vesicles throughout the cytoplasm in cells depleted of Rab8 (supplementary material Fig. S1E,F). Furthermore, there was almost no accumulation of Tfn-R in protrusions. This indicates that Rab8 activity is essential for directing Tfn-R to the pericentriolar region and to cell surface protrusions. We could not see clear differences in the plasma membrane localization of Tfn-R on control versus Rab8-depleted cells. However, the

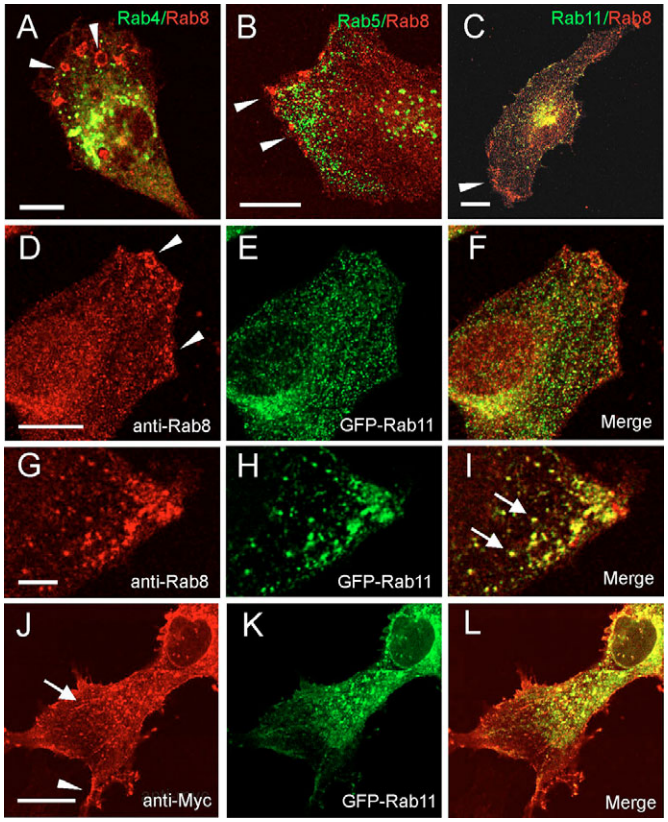

Fig. 2. Rab8 colocalizes with Rab11, but not with Rab4 or Rab5. HT1080 cells expressing EGFP-Rab4, EGFP-Rab5 and EGFP-Rab11 (A-C; green) and endogenous Rab8 (red) were analyzed by confocal microscopy (merge pictures). Endogenous Rab8 (D,G) in HeLa cells expressing EGFP-Rab11 (E,H) colocalizes sometimes on vesicular structures (arrows). F and I are merge pictures. Arrowheads indicate Rab8-positive vacuoles, vesicles and tubules at the leading edge. A HT1080 cell expressing GFP-Rab11 (K) and myc-Rab8-Q67L (J) show a prominent protrusion with Rab8 on tubules (arrow), the plasma membrane and in ruffles (arrowhead). Colocalization is seen on vesicles (L). Bars, 20 μM (A-D,J), 5 μM (G).

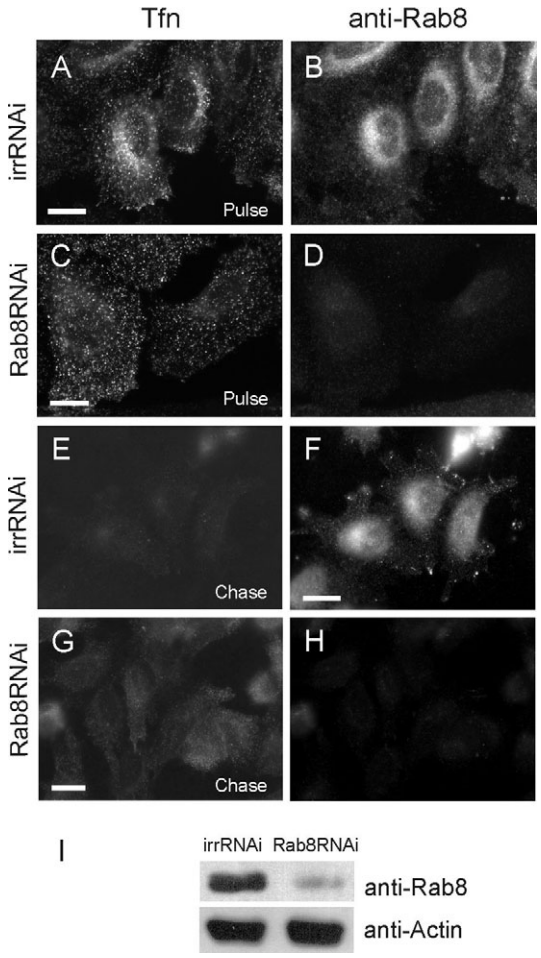

Fig. 3. A role in transferrin recycling for Rab8. Hela cells were transfected with control (A,B,E,F) or Rab8-specific (C,D,G,H) RNAis for 48 hours. Alexa-transferrin was applied to serum starved cells for 30 minutes at 37° (Pulse) and then chased for 30 minutes at 37°C. Note that transferrin (Tfn) is localized to the perinuclear region in Rab8 expressing cells (A), but randomly in Rab8 depleted cells (C). (I) Total lysates from HeLa cells transfected with control or Rab8-specific RNAis were analyzed by western blotting by anti-actin and anti-Rab8 antibodies. Bars, 20 μM.

Rab8-depleted Hela cells were more symmetric and showed contact inhibition, whereas the control cells were asymmetric and grew on top of each other (supplementary material Fig. S1G,H). Expression of Rab8-Q67L induced accumulation of Tfn-R in the perinuclear region where Tfn-R colocalized with Rab8-Q67L (supplementary material Fig. S3A-C). By contrast, Rab8-T22N showed no clear colocalization with Tfn-R and in these cells Tfn-R had a more peripheral localization (supplementary material Fig. S4D-F). Thus, activation of Rab8 seems to be important for the transport of both Tfn and Tfn-R to the cell center.

The cholera toxin B subunit (CTxB) binds to the glycosphingolipid GM1 through which it is endocytosed via the Golgi complex to the ER (Kirkham et al., 2005). To see whether Rab8 is essential for the transport of CTxB to the Golgi complex we applied Alexa-594 conjugated CTxB to cells that have been treated with either control RNAi or the Rab8-specific RNAi (Fig. 4). After a 30 minute chase period about 80% of the cells treated with the control RNAi showed Golgi-specific staining, while only 15% of the cells treated with Rab8-specific RNAi had CTxB accumulated in the Golgi complex. In the Rab8-depleted cells there was more CTxB on the plasma membrane and in small peripheral vesicles (Fig. 4G). A longer chase period increased the Golgi-accumulation of CTxB in depleted cells indicating that Rab8 does not inhibit the transport but retards it (data not shown). Partial colocalization of CTxB and Rab8 on vesicles and tubules was also seen indicating that CTxB passes through the Rab8 pathway (supplementary material Fig. S3J-L).

Rab8 activity is coupled to a tubular compartment

We were able to study the localization of Rab8 in different cell lines because our affinity purified anti-Rab8 antibodies were sensitive enough to detect endogenous Rab8. (Fig. 5). HeLa

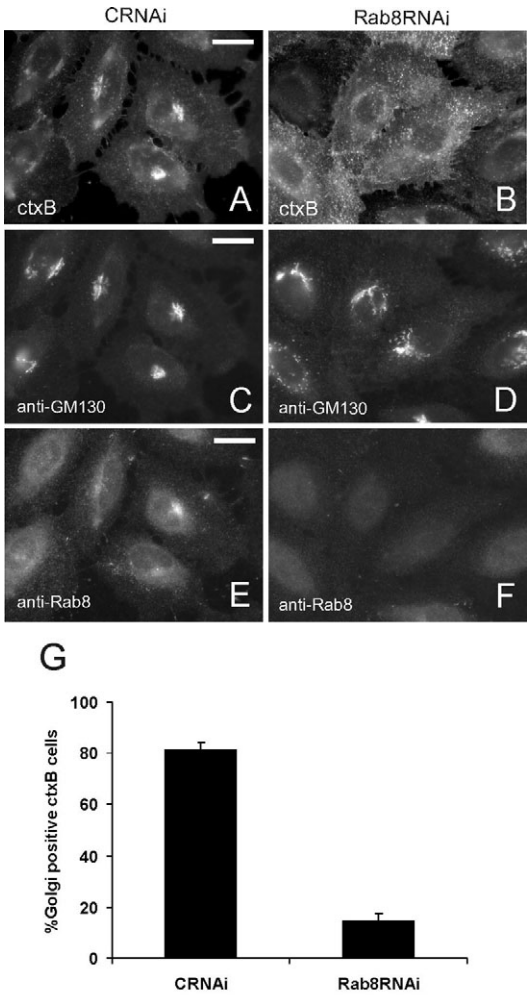

Fig. 4. Rab8 affects cholera toxin B trafficking. Hela cell were treated with control (A,C,E) or Rab8-specific (B,D,F) RNAis for 48 hours. Alexa-595 cholera toxin were bound to the cells on ice for 30 minutes, and then CTxB was allowed to progress to the Golgi apparatus for 30 minutes at 37°C. The cells were fixed and stained for anti-GM130 (C,D) and anti-Rab8 (E,F). The percentage of cells showing CTxB-staining in Golgi was calculated for the cells treated with control RNAi contra Rab8-specific RNAi (G). Values from three separate experiments are shown as the mean ±s.e.m. 60 cells were counted per category and experiment. Bars, 20 μM.

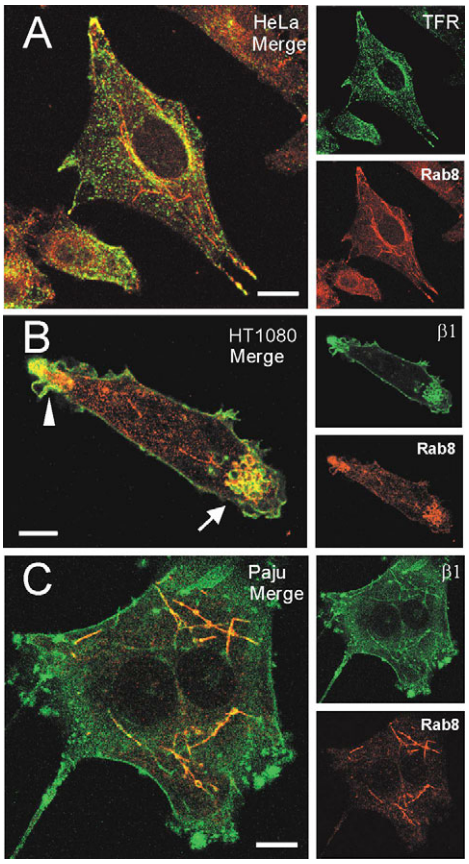

Fig. 5. Rab8 localizes to a tubular compartment. Confocal localization of endogenous Rab8 with β1 integrin and transferrin receptor in three different human cell lines; HeLa carcinoma (A), HT1080 fibrosarcoma (B), and Paju neuroblastoma cells (C). HeLa cells contained Rab8-specific tubular structures that were negative for the transferrin receptor (A). In the HT1080 cells, Rab8 colocalized with β1 integrins on vacuolar structures in the leading lamella (arrow), and sometimes also in the tail region (arrowhead) (B). Paju cells showed prominent Rab8-specific tubules that were positive for β1 integrins (C). Bars, 10 μm.

cells contained Rab8-positive tubular structures; the tubular structures were negative for the transferrin receptor (Fig. 5A), with occasional colocalization of Rab8 and the transferrin receptor in the perinuclear region (Hattula et al., 2002). In polarized HT1080 cells we also observed large macropinosomes containing both Rab8 and β1 integrins at the leading edge, and in the tracking tail (Fig. 5B). The tubular structures were not specific for HT1080 cells but were also present in a human neural cell line (Paju) (Fig. 5C), Huh7, green monkey COS-7, and canine MDCK cells. However, Rab8 was not found in fibroblast-like cells, such as BHK-21, NIH3T3 and WI39, where Rab8b was present. This was also confirmed by RT-PCR (data not shown).

Constitutively active Rab8-Q67L (GFP- or myc-tagged) colocalized with β1 integrins on intracellular vesicles and on large tubular structures in transient and stable transfectants as shown for endogenous Rab8 (supplementary material Fig. S2A,B). The tubular structures were approximately 10-30 μm in length, and extended into cell protrusions. Dominant-negative Rab8-T22N (GFP- or myc-tagged) showed reduced colocalization with β1 integrins, instead β1 integrins accumulated in large vacuoles that were surrounded by a reticular structure containing the dominant-negative Rab8-T22N (supplementary material Fig. S2C). Co-expressing the dominant-negative Rab8-T22N with the constitutively active Rab8-Q67L inhibited the formation of the cell surface extensions and tubular structures normally induced by Rab8-Q67L (data not shown). These results indicate that the formation of cell surface extensions is coupled to the activity of a Rab8/β1 integrin-positive tubular membrane compartment.

Rab8-specific membrane transport from and to the leading edge

Rab8 has been regarded as a regulator of exocytosis (Huber et al., 1993). However, our finding that Rab8 is also found on large tubular structures and on macropinosomes raises questions about the actual membrane traffic route of Rab8. To unravel the nature of the Rab8-specific route we followed the transport of GFP-Rab8 or GFP-Rab8b in live cells. HT1080 cells expressing GFP-Rab8-Q67L are highly polarized with a clear leading edge and show strong protrusive activity by formation of filopodia, lamellipodia and ruffles. By time-lapse video microscopy we saw that membrane ruffling at the leading edge is associated with the formation of Rab8-67L positive macropinosomes and vesicles that are transported inwards to the cell center (Fig. 6A; supplementary material Movie 1). The macropinosomes are closely associated with tubular structures, and sometimes smaller vesicles are seen to fuse with these tubules. The tubules are also seen to independently attach to and detach from the plasma membrane. In addition, there was traffic of rapidly moving small vesicles from the cell center toward the leading edge, probably representing recycling vesicles, but due to their small size they were more difficult to observe (Fig. 6A,C; supplementary material Movies 1 and 2). In motile NIH3T3 cell GFP-Rab8b-wt was predominantly seen on membrane ruffles and on dynamic tubular structures that formed at the ruffling area (Fig. 6B; supplementary material Movie 2). The tubules moved mostly to the cell center, although sometimes they also moved in a forward direction into protrusions. A closer look at the leading edge showed an example where Rab8-containing membrane is taken in from a ruffling area and then redirected to a large vacuole from which membrane was transported to the leading edge to promote lamellipodia forward movement (Fig. 6C; supplementary material Movie 3). Taken together, we show that Rab8-mediated protrusive activity is associated with membrane recycling at the leading edge.

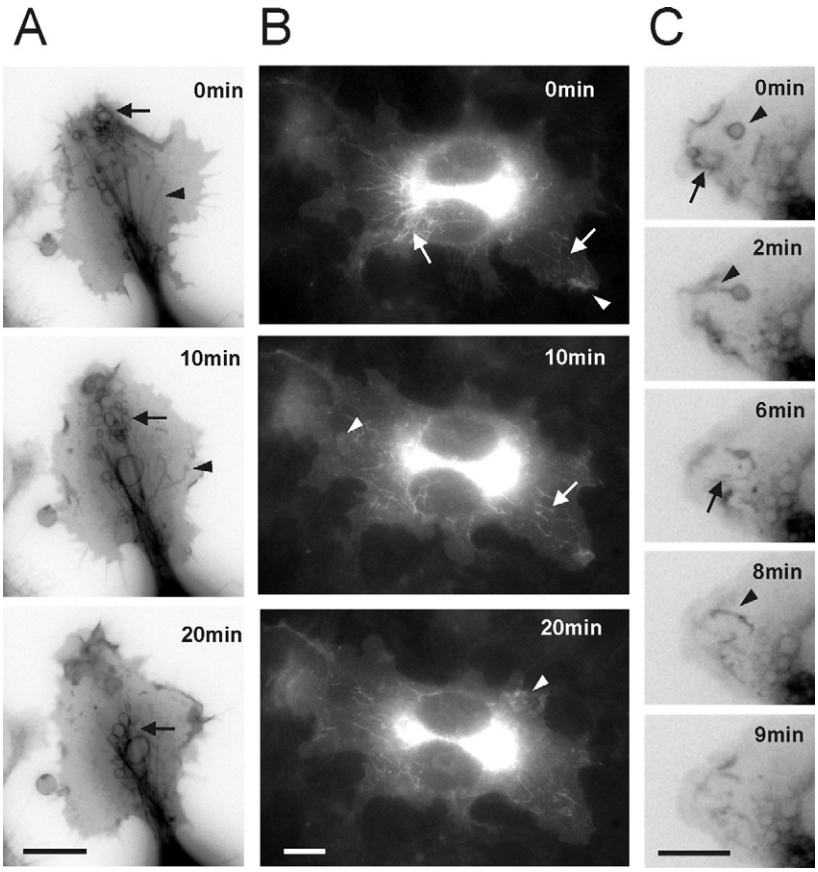

Fig. 6. Rab8-specific membrane turnover at the leading edge. (A) HT1080 cells expressing GFP-Rab8-67L vesicles/vacuoles (arrows) are formed at the leading edge and move toward the cell center. Dynamic tubular structures (arrowheads) are also seen to attach to and retract from the plasma membrane (supplementary material Movie 1). (B) In stably GFP-Rab8b-wt expressing NIH3T3 cells, tubular membrane structures containing GFP-Rab8b-wt are seen forming behind active ruffling lamellipodia (arrowhead), and the tubules are transported to a perinuclear region (arrows) (supplementary material Movie 2). (C) An example of membrane turnover at the leading edge of NIH3T3. GFP-Rab8b-wt positive membranes taken in from a ruffling area (arrow) fuse with a sorting vacuole (arrowhead) that turn into a tubular structure that fuses with the plasma membrane behind the lamellipodia (supplementary material Movie 3). Bars, 10 μM.

Rab8-tubule formation is actin- and microtubule-dependent

About 10% of sparsely seeded HeLa cells contain prominent Rab8-specific tubular structures (Fig. 7K). To see whether tubule formation was dependent on actin dynamics we incubated cells with 0.1 μM cytochalasin D for 30 minutes. We observed a dramatic increase in the number of cells containing tubular structures that stained for endogenous Rab8 (Fig. 7K). Since cytochalasin D depolymerize actin we asked whether RhoA mediated polymerization of actin would have an effect on tubule formation and Rab8 distribution. HeLa cells were transfected with either the dominant-negative GFP-RhoA-T19N or constitutively active GFP-RhoA-G14V (promotes actin stress fiber formation), and then treated with cytochalasin D (Fig. 7A-D). GFP-RhoA-T19N had no effect on the formation of Rab8-specific tubules, whereas RhoA-G14V had a negative effect on the formation of these structures. In GFP-RhoA-G14V cells the tubules were replaced by vesicular structures that were mainly perinuclear. In cells not treated with cytochalasin D GFP and GFP-RhoA-T19N expressing cell showed Rab8 accumulating in cell protrusions, whereas in GFP-RhoA-G14V expressing cells Rab8 was redistributed into a perinuclear region (supplementary material Fig. S4). There was also a slight reduction of the number of cells exhibiting tubules after RhoA-G14V treatment (not shown). Thus, actin polymerization and depolymerization are critical in the biogenesis of Rab8-specific tubules and in the polarized distribution of Rab8 to cell protrusions. To see if microtubules are needed for the formation of Rab8-specific tubules we pre-treated cells with nocodazole for 30 minutes and incubated the cells with both nocodazole and cytochalasin D for an additional 30 minutes. In these cells the formation of tubules was strongly inhibited, and Rab8 re-localized to a perinuclear region (supplementary material Fig. S4G,H). The relocalization of Rab8 to a perinuclear region after both RhoA-G14V expression and microtubule disruption was associated with inhibition of protrusion formation indicating that Rab8 translocation to the cell periphery is coupled to protrusion formation.

To understand how Rab8-specific tubules are formed after addition of cytochalasin D, live cells expressing either GFP-Rab8-wt or GFP-Rab8b-wt were imaged. Non-motile cells lacking endogenous tubules were chosen to better observe the effect of CD. In NIH3T3 cells GFP-Rab8b-wt was first

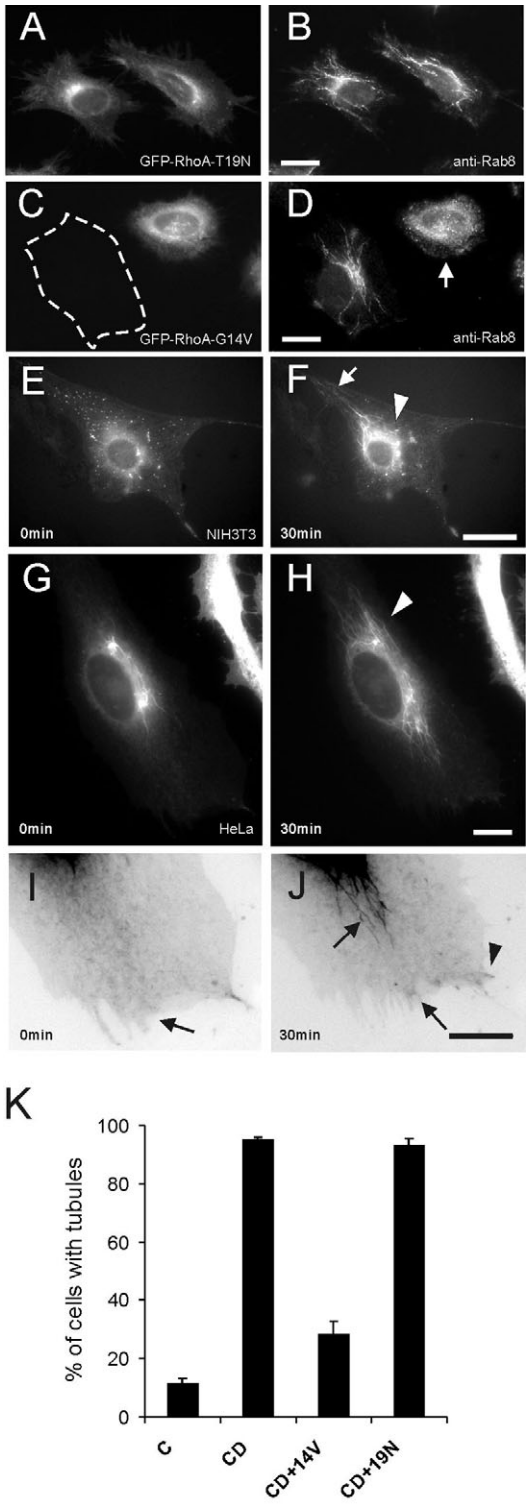

Fig. 7. The formation of Rab8-specific tubular structures is actin- and RhoA-dependent. HeLa cells were transfected overnight with plasmids containing either pEGFP-RhoA-T19N (A,B) or pEGFP-RhoA-G14V (C,D) at 37°C. The transfectants were then incubated in 0.1 μM cytochalasin D (CD) for 30 minutes at 37°C. The cells were fixed, processed for immunofluorescence and stained to detect endogenous Rab8. RhoA proteins were detected through GFP fluorescence. Note that expression of RhoA-T19N did not inhibit CD induced formation of Rab8-specific tubules, whereas RhoA-G14V did (arrow). (K) Quantification of cells containing Rab8-specific tubular structures after CD-treatment, in the absence or presence of GFP-RhoA-G14V and GFP-RhoA-T19N. CD indicates untransfected cells that obtained cytochalasin D. C indicates cells in the absence of CD. A total of about 50 cells were counted per experimental condition. Values, given as percentage of cells (n=50) exhibiting Rab8-specific tubules in each scoring category, from three separate experiments are shown as the mean ±s.e.m. Formation of GFP-Rab8b-wt (NIH3T3; E,F) and GFP-Rab8-wt (Hela; G-J) tubular structures (arrows) were seen after cytochalasin D treatment (30 minutes) (supplementary material Movies 4-6). GFP-Rab8 and GFP-Rab8b vesicles formed at the cell periphery (arrows) and fused to a tubular network in the cell center (arrowhead). There is also an anterograde transport of small Rab8-specific vesicles to the outermost region of the cell, and into forming and retracting filopodia (arrowhead) (I and J; supplementary material Movie 6). Bars, 20 μM (A-F), 10 μM (G-J).

observed on small vesicular structures scattered around the cytoplasm (Fig. 7E; supplementary material Movie 4). After addition of CD, small and larger tubular structures were formed in the periphery of the cell and rapidly transported to a perinuclear region where they fused into a tubular network (Fig. 7F; supplementary material Movie 4). Similar observations were made in HeLa cells expressing GFP-Rab8-wt and treated with CD (Fig. 7G-H, supplementary material Movie 5). In these cells we also looked closer on the region at the plasma membrane and could observe small vesicles budding from the plasma membrane forming into larger tubules or fusing with already existing tubules (Fig. 7I-J, supplementary material Movie 6). This membrane internalization took place in the cell periphery and was associated with retraction of cell protrusions. Interestingly, we also saw rapid transport of vesicles to the cell periphery, where the vesicles entered and fused with forming filopodia, indicating that Rab8 is found on both outgoing and incoming vesicles (Fig. 7I,J; supplementary material Movie 6). In conclusion, our data show that actin and microtubules are essential for the formation of Rab8-specific tubules.

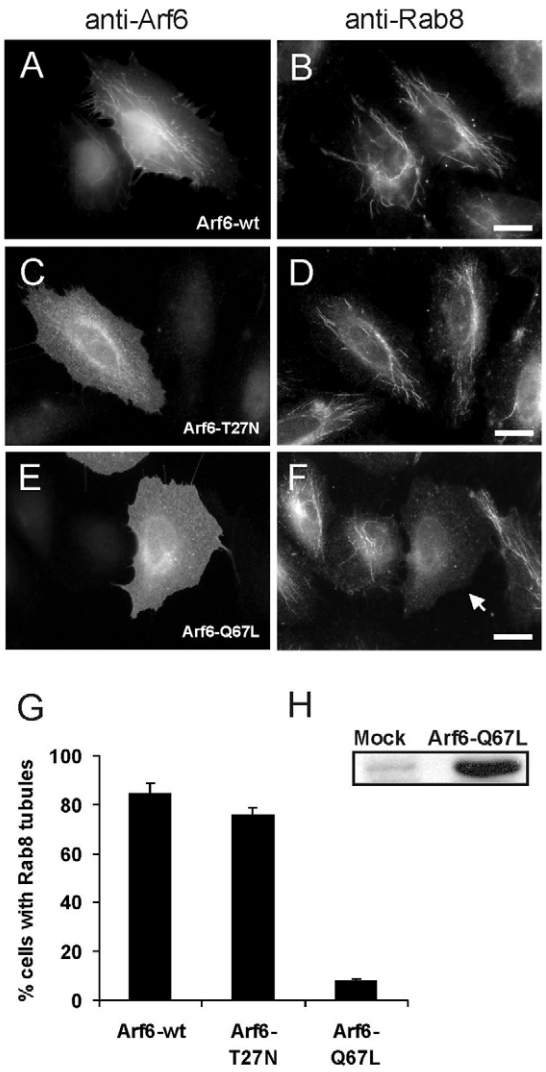

Fig. 8. Arf6 is linked to the formation of Rab8-tubules. HeLa cells were transfected with constructs expressing Arf6-wt (A,B), Arf6-T27N (C,D) or Arf6-Q67L (E,F). Next day the transfectants were incubated in 0.1 μM cytochalasin D (CD) for 30 minutes at 37°C. The cells were fixed, processed for immunofluorescence and stained to detect endogenous Rab8 and recombinant Arf6. Note the absence of tubules in the Arf6-Q67L expressing cell (arrow) (E,F). (G) Quantification of cells containing Rab8-specific tubular structures after CD-treatment, in the presence of Arf6-wt, Arf6-T22N and Arf6-Q67L were done. A total of about 50 cells were counted per experimental condition. Values, given as percentage of cells (n=50) exhibiting Rab8-specific tubules in each scoring category, from three separate experiments are shown as the mean ±s.e.m. (H) The specificity of the anti-Arf6 antibody was tested by immnuoblotting against mock-transfected and Arf6-Q67L transfected total cell extracts. Bars, 20 μM.

Arf6 and Rab8 define a common recycling pathway

Arf6 is known to regulate clathrin-independent internalization and recycling of membranes through an actin-dependent pathway, and Arf6-positive tubular structures form when cells are treated with cytochalasin D (Brown et al., 2001; Radhakrishna and Donaldson, 1997). Treatment of Arf6-wt transfected HeLa cells with 0.1 μM cytochalasin D lead to colocalization of Arf6-wt with endogenous Rab8 on tubular structures, suggesting that Arf6 and are found on same tubular structures (Fig. 8A,B). Moreover, anti-MHCI antibodies were internalized to Rab8-specific tubules as earlier shown for Arf6 (Brown et al., 2001) (supplementary material Fig. S3G-I). Cells expressing the dominant-negative mutant of Arf6(T27N) also showed prominent formation of Rab8-specific tubules after CD treatment, whereas expression of the constitutively active mutant of Arf6(Q67L) strongly inhibited the formation of Rab8-tubules (Fig. 8C-F). In Arf6-Q67L cells Rab8-tubules were mostly absent or found fragmented as small vesicles. Since expression Rab8-Q67L promotes the formation of long cell protrusions we wanted to see whether co-expression of Arf6 proteins with Rab8-Q67L affects the protrusion formation in HT1080 cells (Fig. 9A,B). We found that Arf6-wt and Rab8-Q67L localized to tubular structures in the leading lamella in cells with prominent cell surface extensions. Arf6-T27N and Rab8-Q67 colocalized on vesicles and tubules, and Arf6-T27N partially inhibited the formation of Rab8-Q67L-induced cell surface extension. Arf6-Q67L promoted accumulation of large vacuoles and rounding up of cells, as described earlier for other cell lines (Brown et al., 2001; Santy, 2002). Arf6-Q67L also inhibited Rab8-Q67L-induced cell surface extensions and redistributed Rab8-Q67L to the perinuclear region, Rab8-T22N's usual location. This suggests Arf6-Q67L inhibits membrane from reaching the Rab8-specific recycling compartment. Taken together, these data indicate that both Arf6 and Rab8 participate in the formation of recycling tubules and cell protrusions.

JFC1 is a Rab8- and Rab27a-specific effector

To find new Rab8-specific effector molecules we used Rab8-wt as bait to screen a human kidney yeast two-hybrid cDNA library (Hattula and Peränen, 2000). We found several identical clones that corresponded to the open reading frame encoding the human JFC1 protein, the human homolog of the mouse synaptotagmin-like protein 1 (Slp1) (Fukuda and Mikoshiba, 2001; MacAdara-Berkowitz et al., 2001). JFC1 specifically interacted with wild-type Rab8 and the active GTP-bound

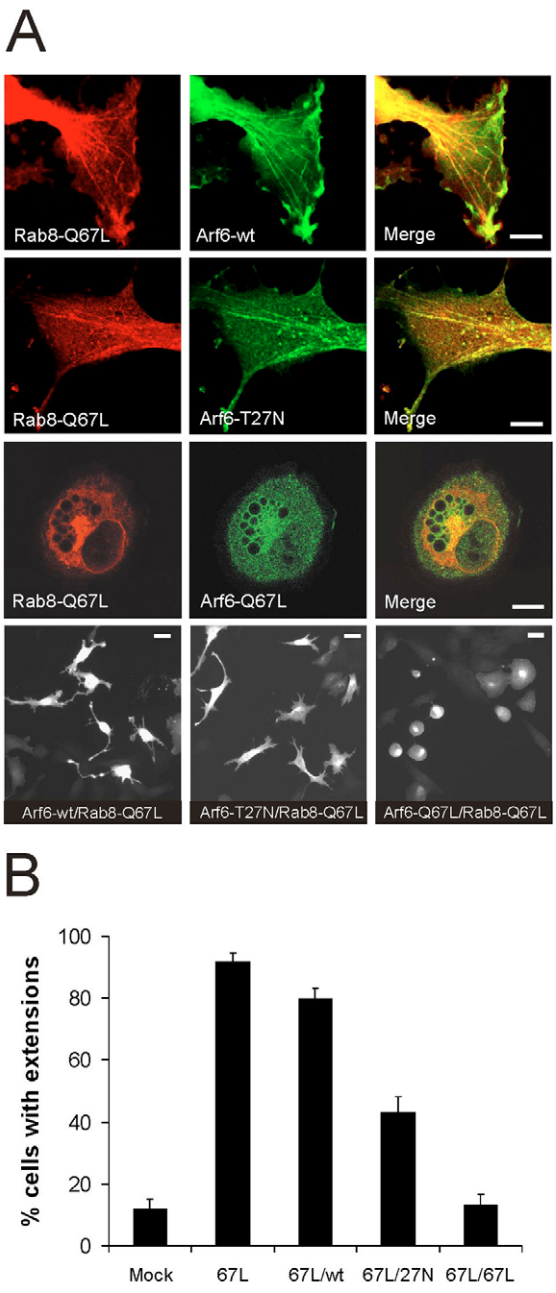

Fig. 9. (A) Arf6 and Rab8 co-operate in inducing cell protrusions. Co-expression studies of Rab8-Q67L and Arf6-wt, Rab8-Q67L and Arf6-T27N, and Rab8-Q67L and Arf6-Q67L in HT1080 cells. Confocal microscopy showed that Rab8-Q67L/Arf6-wt expressing cells contain cell extensions, with Arf6/Rab8-specific tubular structures entering ruffling lamella. Rab8-Q67L and Arf6-T27N colocalized on vesicular and tubular structures. Co-expression of Arf6-Q67L and Rab8-Q67L resulted in the formation of spherical cells, where Arf6-Q67L was localized on large vacuolar structures, and Rab8-Q67L in the perinuclear region. (B) Arf6 cross-talks with Rab8 in the formation of cell surface extensions. HT1080 cells were mock-transfected or transfected with a construct encoding Rab8-Q67L. Co-transfection was done with constructs expressing Arf6-wt/Rab8-Q67L, Arf6-T27N/Rab8-Q67L and Arf6-Q67L/Rab8-Q67L. Cells showing neurite-like extensions were calculated as extension-positive. A total of about 50 cells were counted per experimental condition. Values, given as percentage of cells exhibiting cell surface extension in each scoring category, from three separate experiments are shown as the mean ±s.e.m. Representative fields of these cells are seen in the lowest row of A. Bars, 10 μM, 20 μM (lower panel).

mutant Rab8-67L, but not with the dominant-negative GDP-bound mutant Rab8-22N (Fig. 10A). By contrast, the JFC1 bound to both mutants (T23N and Q78L) of Rab27a, but not to Rab2-Q65L or to laminin (Fig. 10A). Using in vitro binding assays we confirmed the specific interaction of Rab8 to JFC1 (Fig. 10C). In this assay Rab8 bound more efficiently JFC1 than Rab27a, and with higher specificity. Moreover, GST-JFC1 precipitated very efficiently endogenous Rab8, GFP-Rab8-Q67L from cell lysates, but not GFP-Rab8-T22N (Fig. 10D). A co-transfection approach was used to show in vivo interaction of JFC1 to Rab8 (Fig. 10E) (Chen et al., 2002). In the transfected cells JFC1 is produced together with GST, GST-Rab8-T22 or GST-Rab8-Q67L. Precipitation of the extracted proteins with glutathione-Sepharose beads resulted only in precipitation of JFC1 by the GST-Rab8-Q67L protein. Thus, JFC1 shows a clear specificity for Rab8-GTP in vivo. When Hela cells were transfected with constructs encoding GFP-JFC1 or myc-JFC1 we frequently observed JFC1 colocalizing with Rab8 on tubular structures (Fig. 10B). To unravel the possible role of JFC1 in tubule formation we treated GFP and GFP-JFC1 expressing cells with cytochalasin D (supplementary material Fig. S5). We observed that expression of GFP-JFC1, in contrast to GFP, increased the association of Rab8 with vesicles and tubules, and this was associated with a decrease in the number of Rab8-specific tubules, and in an increase in the number of Rab8-specific vesicles and vacuoles (supplementary material Fig. S5).

Discussion

In free moving cells endogenous Rab8 is associated with cell protrusions but when cells form contacts Rab8 re-localizes to a diffuse perinuclear region (Hattula et al., 2002). The Rab8-specific GEF (Rabin8) associates with actin containing lamellipodia and ruffle-like structures at the plasma membrane indicating that Rab8 activation occurs there (Hattula et al., 2002). However, whether Rab8 is found on outgoing or incoming vesicular structures is not known.

Here we show that Rab8-specific vesicles and macropinosomes are formed at ruffling area behind the leading edge, from where they move centripetally toward the cell body. The macropinosomes and vesicles fuse to or form tubular structures that are transported back to the plasma membrane to form new cell protrusions. Inhibiting this membrane traffic route, by Rab8-depletion or dominant-negative mutants of Rab8, abolishes protrusive activity by enhancing actin stress fiber formation and cell-cell adhesion. This indicates that Rab8 regulates the formation of dynamic actin containing cell surface structures. The inverse is also true, because actin modulates the formation of Rab8-specific membrane organelles. We show that actin depolymerization by cytochalasin D promotes the formation of Rab8-specific vesicles and tubules in the cell periphery. The tubules accumulated in the cell center and membrane recycling is inhibited, leading to cell retraction. Removal of cytochalasin D restores protrusions and the distribution of Rab8 to the cell

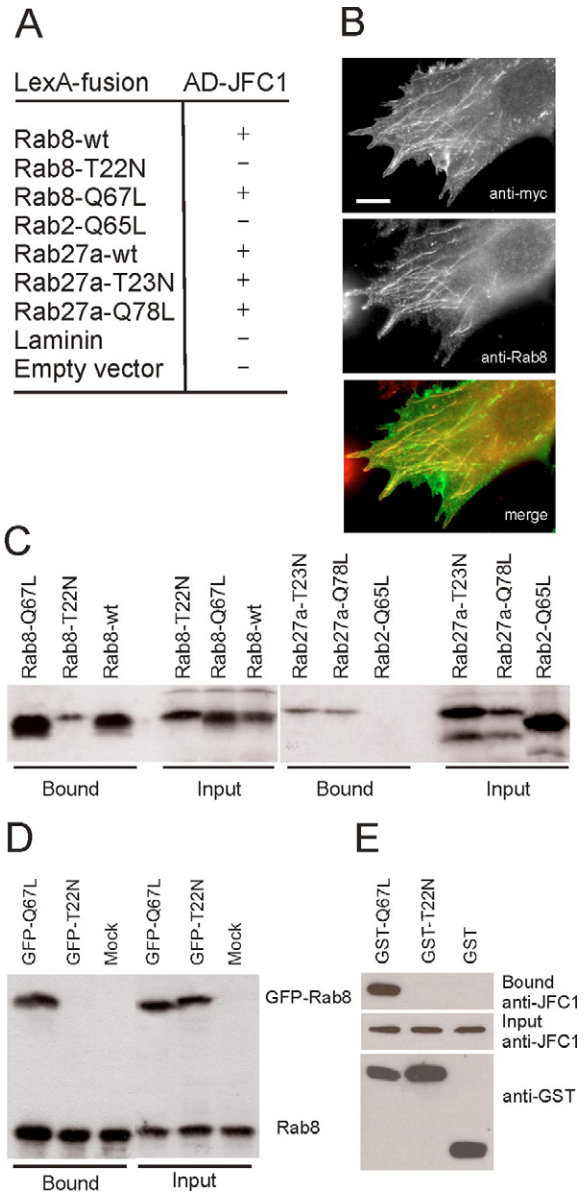

Fig. 10. JFC1 binds specifically to Rab8-GTP. (A) Table showing interactions of JFC1 in the two-hybrid system. Positive interaction (+) is indicated by growth in the absence of leucine and by enhanced β-galactosidase activity using XGal as substrate. (B) Hela cells were transfected by a myc-JFC1 encoding construct, and then the cells were incubated with cytochalasin D for 30 minutes, and stained by anti-myc and anti-Rab8. Endogenous Rab8 colocalizes with myc-JFC1 on tubular structues. (C) In vitro translated Rab2, Rab8, Rab27a and laminin proteins were incubated with GST-JFC1 beads, and bound proteins were analyzed by SDS-PAGE. (D) Cell lysates from cells transfected with contructs encoding GFP-Rab8-Q67L, GFP-Rab8-T22N and mock control were incubated with GST-JFC. Bound proteins were eluted and analyzed by western blotting using anti-Rab8. Note that GST-JFC1 binds GFP-Rab8-Q67L and endogenous Rab8, but not GFP-Rab8-T22N. (E) In vivo binding of JFC1 to Rab8. The construct encoding myc-JFC1 was co-transfected with constructs encoding GST-Rab8-Q67L, GST-Rab8-T22N or GST. Cell lysates from these cells were bound to glutathione-Sepharose beads, and bound proteins were analyzed by westerm blotting with anti-JFC1 and anti-GST antibodies. Only GST-Rab8-Q67L bound JFC1 in vivo. Bar, 10 μM.

periphery (J.P., unpublished). However, we also show that tubule formation is microtubule-dependent, because if microtubules are disrupted before and during treatment with cytochalasin D no Rab8-specific tubules are formed. Thus, microtubules are needed for the formation of the tubules, while actin depolymerization probably initiates the process of tubulation.

The small GTPase Arf6 is also found on tubular structures after actin depolymerization with cytochalasin D, and behaves in many respects like Rab8 (Radhakrishna and Donaldson, 1997; Prignet et al., 2003) (this study). Both Arf6 and Rab8 induce the formation of protrusions (Peränen et al., 1996; Radhakrishna and Donaldson, 1997). It is known that overexpression of Arf6-Q67L results in internalization and trapping of actin-coated vacuoles that are unable to recycle back to the cell surface (Brown et al., 2001). This leads with time to inhibition of both ruffling, endocytosis and cell polarity (Brown et al., 2001; Santy, 2002; Hashimoto et al., 2004). Here we show that Arf6-Q67L also inhibits the formation of Rab8-tubules, and decreases the formation of Rab8-induced cell protrusions. One explanation for this inhibitory action of Arf6 on Rab8 is that Arf6-Q67L acts upstream of Rab8 by inhibiting membrane from reaching the Rab8 recycling compartment. How Arf6 and Rab8 cross-talk is currently under investigation.

It is well established that polarized exocytosis of newly synthesized membrane proteins occurs towards the leading edge in migrating cells (Bergman et al., 1983). In addition, directional recycling of Tfn-R and integrins to the leading edge has been reported (Hopkins et al., 1994; Laukaitis et al., 2001). Rab8 may be a major player in these processes, because activation of Rab8 induces polarized membrane transport of newly synthesized proteins to cell extensions, and Rab8 depletion inhibits delivery of Tfn-R to cell protrusions (Peränen et al., 1996) (this study). Activation of Rab8 also missorts VSV-G to the apical surface domain in MDCK cells, while the dominant-negative mutant of Rab8 has no effect on sorting (Ang et al., 2003). Interestingly, the dominant-negative mutant of Rab8 and Rab8-depletion enhance cell-cell adhesion suggesting that Rab8 activity is perhaps not important in maintaining proper sorting in fully polarized epithelial cells. We have shown that Rab8 is linked to huntingtin via optineurin (Hattula and Peränen, 2000). Sahlender et al. (Sahlender et al., 2005) have demonstrated that optineurin links myosin VI to the Golgi and is involved in Golgi organization and exocytosis. They also found that Rab8 recruits myosin VI onto Rab8-positive vesicles and tubules. Myosin VI is not only found in the Golgi region but also on ruffles, endocytic and secretory vesicles as shown here for Rab8 (Buss et al., 2002). Moreover, Rab8 is essential for the targeting of AMPAR to the spine surface and receptor recycling at the postsynaptic terminal (Gerges et al., 2004). Thus, Rab8 seems to play an important role in targeting molecules to specific cell surface domains.

JFC1 is a member of the synaptotagmin-like protein (Slp) family that contains a Rab-binding domain (RBD) in the amino-terminal and two tandem-C2 domains in the carboxy-terminus. It interacts with Akt, Rab27a and the NADPH oxidase (Johnson et al., 2005a; Johnson et al., 2005b; MacAdara et al., 2001). JFC1 is known to regulate androgen-dependent secretion of prostate-specific antigen and prostatic-specific acid phosphatase (Johnson et al., 2005b). Here, we show that the JFC1 protein not only interacts with Rab27a but

also with Rab8 in a nucleotide specific manner suggesting that these Rab proteins may functionally overlap. This is also supported by the fact that Rab8 and Rab27 colocalize on dense-core vesicles and on melanosomes, and they both participate in the actin-dependent movement of the melanosomes (Chabrillat et al., 2005; Fukuda et al., 2002). Furthermore another Slp (Slp4-a) is also known to bind both Rab8 and Rab27a (Fukuda, 2003). We show that JFC1 colocalizes on tubular and vesicle structures containing endogenous Rab8 suggesting that JFC1 is linked to the Rab8-specific pathway. Moreover, ectopically expressed JFC1 seems to increase the association of Rab8 with tubular and vesicular structures after actin disruption, and this is associated with a decrease in the number of tubules. At the moment we do not know whether overexpression of JFC1 inhibits the transformation of incoming vesicles into tubules or promotes disassembly of existing tubules.

Rab8 also modulates the traffic of incoming cargo molecules. Rab8 partially colocalizes with Rab11 suggesting that it is connected to the endocytic recycling compartment (ERC). However, they seem to control different steps of recycling. Rab11 regulates Tfn recyling from the ERC to the PM, whereas Rab8 controls the transport of Tfn/Tfn-R to the ERC (Ullrich et al., 1996). In Rab8 depleted cells Tfn are seen in small vesicles, probably representing sorting endosomes (SEs). However, Rab8 depletion does not significantly inhibit Tfn recycling, which probably occurs from SEs by a Rab4-dependent pathway. Overexpression of the myosin-Vc tail leads to colocalization with the Tfn-R and Rab8, and also perturbs Tfn trafficking (Rodriguez and Cheney, 2002). Thus, the role of Rab8 might be indirect, perhaps by regulating cytoskeleton-based movement of vesicular structures (Chabrillat et al., 2005) (this study). This is supported by the fact that Rab8 depletion promotes the formation of actin stress fibers, whereas activation of Rab8 has the opposite effect. Rab8 also regulates microtubule dynamics, and its localization is dependent on the integrity of microtubules (Peränen et al., 1996) (this study). Thus, Rab8 might play a role in the organization of the ERC and in facilitating polarized vesicle movement along microtubules to cell surface domains.

Cholera toxin B (CTxB) uses different modes to enter the cell (Shogomori and Futerman, 2001; Massol et al., 2004; Kirkham et al., 2005). We show here that Rab8 depletion inhibits the retrograde transport of CTxB to the Golgi compartment, suggesting that Rab8 functions in a step between the plasma membrane and the Golgi. Arf6, Rab22a and dynamin mutants also inhibit the transport of CTxB to Golgi. (Kirkham et al., 2005; Mesa et al., 2005). The fact that Rab8 colocalizes with Arf6, Rab22b and to some extent with Rab22a indicates that these proteins define a common clathrin-independent pathway through which CTxB is transported (Rodriguez-Gabin et al., 2001) (this study; J.P., unpublished).

How does Rab8 control cell shape? Our results support a model where Rab8 activity is needed to rapidly take in membrane from the cell surface (ruffles) regions that no longer support adhesion. This membrane that contains structural (adhesion receptors) and regulatory (Arf6, Rho and Ras) components is then recycled back to the plasma membrane via a recycling compartment for the formation of new protrusions (Radhakrishna and Donaldson, 1997; Ng et al., 1999; Furuhjelm and Peränen, 2003; Deretic et al., 2004; Powelka et al., 2004; Schlunck et al., 2004). According to this, a shift from exocytosis to endocytosis (macropinocytosis) of membranes would stop protrusive activity and result in retraction of cell surface domains (tracking tail). Thus an appropriate equilibrium between exocytosis and endocytic recycling could be the driving force in the formation and the destruction of cell surface domains. A cessation of this membrane-recycling pathway would promote plasma membrane stabilization and cell-cell adhesion. This process is likely to be evolutionary well preserved because a dominant-negative mutant of the Rab8-like protein of *Dictyostelium discoideum*, Sas1, also promotes cell-cell adhesion (Powell and Temesvari, 2004). Our hypothesis is in accordance with the role of Rab8 in neurite outgrowth and development of photoreceptors (Huber et al., 1995; Kametani et al., 2003; Moritz et al., 2001; Deretic et al., 2004). Future studies should unravel the role of Rab8 in processes like cell polarity, cell migration, epithelial-mesenchymal transition, and cell division.

Materials and Methods

DNA constructs

The pEGFP-Rab8-wt, pEGFP-Rab8-T22N, pEGFP-Rab8-Q67L, pEGFP-Rab8b-wt, pEGFP-Rab8b-T22N, Rab8b-Q67L, pEGFP-RhoA-wt, pEGFP-RhoA-T19N and pEGFP-RhoA-G14V constructs have been previously described (Hattula et al., 2002; Peränen and Furuhjelm, 2000; Vartiainen et al., 2000). pEGFP-Rab8-N121I was constructed as described for the other Rab8 mutants (Peränen and Furuhjelm, 2000). The open reading frames of Rab8-T22N and Rab8-Q67L were also cloned into pcDNA4/TO (Invitrogen) and pIRES (Clontech). The GST-tagged fusions of Rab8 were obtained by cloning Rab8-T22N and Rab8-Q67L into the pEBG-SrfI vector (Chen et al., 2002). The human Rab4, Rab5, Rab11 coding regions were amplified from human kidney cDNA by specific primers, and cloned into pGEM-1 (Promega) and pEGFP-C1 vectors (Clontech). The human Rab27a was similarly cloned into pGEM-1, and site-directed mutagenized to create pGEM-Rab27a-T23N and pGEM-Rab27a-Q78L. Arf6-wt was amplified by PCR from human muscle cDNA and site-directed mutagenized to obtain Arf6-T27N and Arf6-Q67L. The Arf6 genes were cloned into pGEM-1, pcDNA4/TO, and pEGFP-N1 (Clontech). The open reading frame of JFC1 was cloned into pEGFP-C1, pcDNA4/TO, and pGEX-2T (Amersham). All amplified genes were sequenced to confirm that no mutations had been introduced during PCR. Details on the constructs are available upon request.

Yeast two-hybrid screen

The Rab8-wt gene was used as bait to screen a human kideney cDNA yeast two-hybris library for possible Rab8 effectors as previously described (Hattula and Peränen, 2000). The full-length open reading frame of JFC1 was cloned into pB42AD (Clontech) and was tested against Rab8, Rab2, Rab27a and their corresponding mutants that had been cloned into pGilda (Clontech).

Production of JFC1 antisera

GST-JFC1 was expressed in *E. coli* at 15°C, purified on glutathione beads and immunized into rabbits as described previously (Peränen and Furuhjelm, 2000). Affinity purification of antibodies was done by using nitrocellulose strips containing GST-JFC1 (Peränen et al., 1996).

Stable cell lines and transient transfections

HT1080 fibrosarcoma cells were grown and maintained in MEM-medium supplemented with 10% (v/v) fetal bovine serum (Gibco BRL). To obtain stable cell lines, HT1080 cells were grown on 100 mm plates and transfected with 10 μg of pIRES (control), pIRES-Rab8-T22N, pIRES-Rab8-Q67L, pEGFP (control), pEGFP-Rab8-T22N or pEGFP-Rab8-Q67L plus 40 μl each of Lipofectamine in Optimem™ (Gibco BRL). Cells were split the next day and plated at different dilutions in medium containing 700 μg ml^{-1} G418. Clones were collected 12 days later and the presence of the Rab8 proteins was immunologically confirmed. The cell morphology of stable cell lines was monitored at low magnification (25×) after fixing the cells with 4% paraformaldehyde and staining with aqueous 1% crystal violet. Stable NIH3T3 transfectants expressing GFP-Rab8b-wt were obtained similarly. The growth conditions for the HeLa and Paju cells were as described earlier (Peränen and Furuhjelm, 2000; Zhang et al., 1996). To study the influence of Rab8 on cell morphogenesis we transfected HT1080 cells with Rab8 constructs alone or together with different Arf6 constructs in a molar ratio of 1:1. Fugene 6 (Boehringer Mannheim) was used as transfection reagent, and all cells were studied 20 hours after transfection. Cells containing neurite-like surface extensions longer

than one cell body were considered extension-positive. Quantifications were done by examining a total of 50 cells from three independent experiments, and data were mean ± s.d.

Knockdown of Rab8 by RNA interference

The target sequence used for synthesizing Rab8-specific RNAi was GACAAGTTTCCAAGGAACG (Schuck et al., 2004), and the sequence for the corresponding control RNAi was AGCTTCATAAGGCGCATGC (Bertling et al., 2004). Hela cells were seeded in 35 mm plates 1 day prior to transfection. Semi-confluent cells were transfected using the magnet assisted transfection kit (MATra, IBA, Göttingen, Germany). In brief, 60 pmol of siRNA synthesized by Dharmacon (Lafayette, CO) was mixed into 500 μl of Optimem^{TM}. Then 1 μl of MATra beads were added to the 500 μl, mixed, and incubated at room temperature for 30 minutes. Next, 500 μl of growth medium from the cell plate was removed and replaced with the MATra/siRNA solution, and mixed. The cell plates with the transfection mix were placed on a magnetic plate for 15 minutes at 37°C in a cell incubator. After 4 hours in the incubator the cells obtained fresh growth medium, and were grown for 2 days before assaying Rab8 depletion.

Cholera toxin and transferrin uptake

The cholera toxin uptake was performed essentially as described by Hölttä-Vuori et al. (Hölttä-Vuori et al., 2000). In brief, cells that had been treated for 2 days by either control RNAi or Rab8-specific RNAi (see above) were incubated with 1 μg ml^{-1} Alexa 594-conjugated cholera toxin (CTxB; Molecular Probes) in serum-free culture medium (MEM) for 30 minutes on ice. After washing three times with serum-free medium supplemented with 0.02% BSA, the cell were incubated in the same medium for 30 minutes at 37°C and fixed. To quantify the fraction of CTxB not associated with Golgi, the fraction of cells where CTxB colocalized with the Golgi marker anti-GM130 (BD transduction), stained by anti-mouse IgG allophycocyanin (Molecular Probes), were subtracted and the result expressed as a percentage of total number of cells.

Two days after Rab8-depletion cells grown on coverslips in 35 mm plates were washed in serum-free DMEM supplemented with 0.2% BSA and preincubated for 2 hours at 37°C in serum-free medium. The cells were then incubated with 10 μg ml^{-1} alexa488-transferrin in serum-free medium (Molecular Probes) for 30 minutes at 37°C (pulse). The cells were then washed twice with DMEM supplemented with 10% FCS, and then incubated in the same medium for 30 minutes at 37°C (chase). The cells were rinsed for 45 seconds with 0.5% acetic acid, 0.5 M NaCl pH 3.0 to remove Tfn from the cell surface, washed three times with PBS, fixed with paraformaldehyde and processed for immunofluorescence as described previously (Peränen et al., 1996). Incubation of HeLa cells with anti-MHCI antibodies (W6/32; Novocastra) were as previously described (Naslavsky et al., 2004).

Western blotting

Lysates from stable cell lines and Rab8-depleted cells were run on SDS-PAGE and transferred to nitrocellulose as described (Peränen et al., 1996). Rab8 was detected by a monoclonal anti-Rab8 antibody (code 66320, BD transduction) or an affinity purified anti-Rab8 (Peränen and Furuhjelm, 2000). GST-fusions were detected by anti-GST (Cell Signalling Technology). The secondary antibodies were goat anti-mouse HRP or anti-rabbit HRP (Jackson), and detection was by ECL (Amersham).

In vitro and in vivo binding assays

Recombinant GST-JFC1 was expressed in *Escherichia coli* strain BL21(DE3), and purified onto gluathionine Sepharose® beads (Amersham) according to the manufacturer (Amersham). Rab2, Rab8-wt. Rab8-T22N, Rab8-Q67L, Rab27a-T23N and Rab27a-Q78L were translated in vitro from corresponding plasmids using a TNT Quick kit (Promega) according to the manufacturer's instructions. The in vitro translation products were then incubated with GST-JFC1 attached to glutathione-Sepharose® beads as previously described (Hattula and Peränen, 2000). In vivo produced GFP-Rab8 was also used for binding assays. Briefly, Hela cells expressing GFP-Rab8-T22N or GFP-Rab8-Q67L were lysed in binding buffer (50 mM Tris pH 7.5, 150 mM NaCl, 2 mM $MgCl_2$, 1% Triton X-100). The lysate was cleared by centrifugation (15,000 ***g***, 15 minutes, +4°C). The cleared lysate was incubated with GST-JFC1 beads for 2 hours at 4°C. The beads were washed four times with the incubation buffer during 30 minutes. Bound material was eluted from the beads with Laemmli sample buffer and loaded onto a 12% SDS-polyacrylamide gel. As a control, 1/5 of the input in vitro material was also loaded onto the gel. Bound and input material was assayed by western blot using anti-Rab8 antibody (code 66320, BD transduction) as described above.

In vivo binding was done by co-transfection of pcDNA-mycJFC1 with pEBG-*Srf*I, pEBG-Rab8-T22N or pEBG-Rab8-Q67L in HEK293 cells using Fugene 6 according to the manufacturer (Roche). One day latter the cells from a 5 cm plates were homogenized in a buffer containing 30 mM Tris-HCl pH 7.5, 150 mM NaCl, 1.0% Triton-X 100, 0.5 mM GTPγS and 0.4 mM PMSF and solubilized for 20 minutes at 4°C. Insoluble material was removed by centrifugation at 15,000 ***g*** for 15 minutes. The obtained supernatant was incubated with glutathione-Sepharose beads (30 μl beads) at 4°C for 2 hours. The beads were washed four times with 30 mM Tris-HCl pH 7.5, 150 mM NaCl, 0.2% Triton-X 100, and 0.4 mM PMSF. The bound proteins were eluted by Laemmli sample buffer, and subjected to 12% SDS-PAGE, followed by immunoblotting with anti-JFC1 antibodies as described above. To detect GST, GST-Rab8-T22N and GST-Rab8-Q67L the blot was stripped and reprobed with anti-GST (Cell Signaling).

Immunofluorescence and confocal microscopy

Cells were grown on coverslips, fixed with 4% paraformaldehyde, permeabilized with 0.1% Triton X-100 and processed as described (Peränen et al., 1996). The anti-Rab8 rabbit antiserum was affinity purified as previously described (Peränen et al., 1996; Peränen and Furuhjelm, 2000). Other antibodies used were anti-Arf6 (6ARF01; Neomarkers), anti-β1-integrin (clone P4C10; Gibco BRL), anti-transferrin receptor (Roche), anti-myc (Roche), anti-γ-catenin (TransLab). The secondary antibodies were goat anti-rabbit IgG lissamine rhodamine, goat anti-mouse IgG lissamine rhodamine and goat anti-mouse IgG fluorescein isothiocyanate (FITC) from Jackson ImmunoResearch. TRITC-conjugated phalloidin (Molecular Probes) was used to visualize actin. Fluorescence of fixed cells was observed either with the Bio-Rad MRC-1024 confocal system linked to a Zeiss Axiovert 135 M microscope or with an Olympus AX70 fluorescence microscope.

Time-lapse microscopy

Living HeLa, HT1080 and NIH3T3 cells expressing different GFP-Rab8/Rab8b proteins were observed with an inverted IX71 Olympus microscope (Olympus, Tokyo, Japan) through a 40×1.5N objective, equipped with a Polychrome IV monochromator (TILL Photonics, Eugene, OR) with appropriate filters. Images were recorded in intervals of 15 or 30 seconds and processed using TILL Imaging system software.

We thank P. Auvinen, S. Falck, and P. Lappalainen and for comments on the manuscript. We also thank L. C. Andersson for the Paju cells. The work was supported by the Academy of Finland, Helsinki University Foundation, Oskar Öflunds Foundation, Jenny and Antti Wihuri foundation and by the Research and Science Foundation of Farmos.

References

Ang, A. L., Fölsch, H., Koivisto, U.-M., Pypaert, M. and Mellman, I. (2003). The Rab8 GTPase selectively regulates AP-1B-dependent basolateral transport in polarized Madin-Darby canine kidney cells. *J. Cell Biol.* **163**, 339-350.

Armstrong, J., Thompson, N., Squire, J. H., Smith, J., Hayes, B. and Solari, R. (1996). Identification of a novel member of the Rab8 family from the rat basophilic leukemia cell line, RBL.2H3. *J. Cell Sci.* **109**, 1265-1274.

Bergmann, J. E., Kupfer, A. and Singer, S. J. (1983). Membrane insertion at the leading edge of motile fibroblasts. *Proc. Natl. Acad. Sci. USA* **80**, 1367-1371.

Bertling, E., Hotulainen, P., Mattila, P. K., Matilainen, T., Salminen, M. and Lappalainen, P. (2004). Cyclase-associated protein 1 (CAP1) promotes cofilin-induced actin dynamics in mammalian nonmuscle cells. *Mol. Biol. Cell* **15**, 2324-2334.

Bretscher, M. S. (1996). Getting membrane flow and the cytoskeleton to cooperate in moving cells. *Cell* **15**, 601-606.

Brown, F. D., Rozelle, A. L., Yin, H. L., Balla, T. and Donaldson, J. G. (2001). Phosphatidylinositol 4, 5-bisphosphate and Arf6-regulated membrane traffic. *J. Cell Biol.* **154**, 1007-1017.

Buss, F., Luszio, J. P. and Kendrick-Jones, J. (2002). Myosin VI, an actin motor for membrane traffic and cell migration. *Traffic* **3**, 851-858.

Chabrillat, M. L., Wilhelm, C., Wasmeier, C., Sviderskaya, E. V., Louvard, D. and Coudrier, E. (2005). Rab8 regulates the actin-based movement of melanosomes. *Mol. Biol. Cell* **16**, 1640-1650.

Chen, P., Hutter, D., Liu, P. and Liu, Y. (2002). A mammalian expression system for rapid production and purification of active MAP kinase phosphatases. *Protein Expr. Purif.* **24**, 481-488.

Deretic, D., Traverso, V., Parkins, N., Jackson, F., Rodriguez de Turco, E. B. and Ransom, N. (2004). Phosphoinositides, ezrin/moesin, and rac1 regulate fusion of rhodopsin transport carriers in retinal photoreceptors. *Mol. Biol. Cell* **15**, 359-370.

D'Souza, C. and Chavrier, P. (2006). ARF proteins: roles in membrane traffic and beyond. *Nat. Rev. Mol. Cell Biol.* **7**, 347-358.

Fukuda, M. (2003). Slp4-a/granuphilin-a inhibits dense-core vesicle exocytosis through interaction with the GDP-bound form of Rab27a in PC12 cells. *J. Biol. Chem.* **278**, 15390-15396.

Fukuda, M. and Mikoshiba, K. (2001). Synaptotagmin-like protein 1-3: novel family of C-terminal-type tandem C2 proteins. *Biochem. Biophys. Res. Commun.* **281**, 1226-1233.

Fukuda, M., Kanno, E., Saegusa, C., Ogata, Y. and Kuroda, T. S. (2002). Slp4-a/Granuphilin-a regulates dense-core vesicle exocytosis in PC12 cells. *J. Biol. Chem.* **42**, 39673-39678.

Furuhjelm, J. and Peränen, J. (2003). The C-terminal end of R-Ras contains a focal adhesion targeting signal. *J. Cell Sci.* **116**, 3729-3738.

Gerges, N. Z., Backos, D. S. and Esteban, J. A. (2004). Local control of AMPA recptor traffickinf at the postsynaptic terminal by a small GTPase of the Rab family. *J. Biol. Chem.* **279**, 43870-43878.

Hashimoto, S., Onodera, Y., Hashimoto, A., Tanaka, M., Hamaguchi, M., Yamada,

A. and Sabe, H. (2004). Requirement for Arf6 in breast cancer invasive activities. *Proc. Natl. Acad. Sci. USA* **101**, 6647-6652.
Hattula, K. and Peränen, J. (2000). FIP-2, a coiled-coil protein, links Huntingtin to Rab8 and modulates cellular morphogenesis. *Curr. Biol.* **10**, 1603-1606.
Hattula, K., Furuhjelm, J., Arffman, A. and Peränen, J. (2002). A Rab8-specific GDP/GTP exchange factor is involved in actin remodelling and polarized membrane transport. *Mol. Biol. Cell* **13**, 3268-3280.
Heat, J. P. and Holifield, B. F. (1991). Cell locomotion: new research tests old indeas on membrane and cytoskeletal flow. *Cell Motil. Cytoskeleton* **18**, 245-257.
Hopkins, C. R., Gibson, A., Shipman, M., Strickland, D. K. and Trowbridge, I. S. (1994). In migrating fibroblasts, recycling receptors are concentrated in narrow tubules in the pericentriolar area, and then routed to the plasma membrane of the leading lamella. *J. Cell Biol.* **125**, 1265-1274.
Hölttä-Vuori, M., Määttä, J., Ullrich, E., Kuismanen, E. and Ikonen, E. (2000). Mobilization of late-endosimal cholesterol is inhibited by Rab guanine nucleotide dissociation inhibitor. *Curr. Biol.* **10**, 95-98.
Huber, L. A., Pimplikar, S., Parton, R. G., Virta, H., Zerial, M. and Simons, K. (1993). Rab8, a small GTPase in vesicular traffic between the TGN and the basolateral plasma membrane. *J. Cell Biol.* **123**, 35-45.
Huber, L. A., Dupree, P. and Dotti, C. G. (1995). A deficiency of the small GTPase rab8 inhibits membrane traffic in developing neurons. *Mol. Cell. Biol.* **15**, 918-924.
Johnson, J. J., Ellis, B. A., Noack, D., Seabra, M. C. and Catz, S. D. (2005a). The Rab27a-binding protein, JFC1, regulates androgen-dependent secretion of prostate-specific antigen and prostatic-specific acid phospatase. *Biochem. J.* **391**, 699-710.
Johnson, J. J., Pacquelet, S., Lane, W. S., Eam, B. and Catz, S. D. (2005b). Akt regulates the subcellular localization of the Rab27a-binding protein JFC1 by phosphorylation. *Traffic* **6**, 667-681.
Kametani, F., Usami, M., Tanaka, K., Kume, H. and Mori, H. (2004). Mutant presenilin (A260V) affects Rab8 in PC12D cell. *Neurochem. Int.* **44**, 313-320.
Kirkham, M., Fujita, A., Chadda, R., Nixon, S. J., Kurzchalia, T. V., Sharma, D. K., Pagano, R. E., Hancock, J. F., Mayor, S. and Parton, R. G. (2005). Ultrastructural identification of uncoated caveolin-independent early endocytic vehicles. *J. Cell Biol.* **168**, 465-476.
Lauffenburger, D. A. and Horwitz, A. F. (1996). Cell migration: a physical integrated molecular process. *Cell* **84**, 358-369.
Laukaitis, C. M., Webb, D. J., Donais, K. and Horwitz, A. F. (2001). Differential dynamics of alpha5 integrin, paxillin, and alpha-actinin during formation and disassembly of adhesions in migrating cells. *J. Cell Biol.* **153**, 1427-1440.
MacAdara-Berkowitz, J. K., Catz, S. D., Johnson, J. L., Ruedi, J. M., Thon, V. and Babior, B. M. (2001). JFC1, a novel tandem C2 domain-containing protein associated with the leukocyte NADPH oxidase. *J. Biol. Chem.* **276**, 18855-18862.
Massol, R. H., Larsen, J. E., Fujinga, Y., Lencer, W. I. and Kirchhausen, T. (2004). Cholera toxin toxicity does not require functional Arf6- and dynamin-dependent endocytic pathways. *Mol. Biol. Cell* **15**, 3631-3641.
Mesa, R., Magadán, J., Barbieri, A., López, C., Stahl, P. D. and Mayorga, L. S. (2005). Overexpression of Rab22a hampers the transport between endosomes and the Golgi apparatus. *Exp. Cell Res.* **304**, 339-353.
Mitchison, T. J. and Cramer, L. P. (1996). Actin-based cell motility and cell locomotion. *Cell* **84**, 371-379.
Moritz, O. L., Tam, B. M., Hurd, L. L., Peränen, J., Deretic, D. and Papermaster, D. S. (2001). Mutant rab8 Impairs docking and fusion of rhodopsin-bearing post-Golgi membranes and causes cell death of transgenic Xenopus rods. *Mol. Biol. Cell* **12**, 2341-2351.
Naslavsky, N., Weigert, R. and Donaldson, J. G. (2004). Charcterization of a nonclathrin endocytic pathway: membrane cargo and lipid requirements. *Mol. Biol. Cell* **15**, 3542-3552.
Ng, T., Shima, D., Squire, A., Bastiaens, P. I., Gschmeissner, S., Humphries, M. J. and Parker, P. J. (1999). PKCα regulates β1 integrin-dependent cell motility through association and control of integrin traffic. *EMBO J.* **18**, 3909-3923.
Nobes, C. D. and Hall, A. (1999). Rho GTPases control polarity, protrusion, and adhesion during cell movement. *J. Cell Biol.* **144**, 1235-1244.
Palacios, F., Price, L., Schweitzer, J., Collard, J. G. and D'Souza-Schorey, C. (2001). An essential role for Arf6-regulated membrane traffic in adherens junction turnover and epithelial cell migration. *EMBO J.* **20**, 4973-4986.
Peränen, J. and Furuhjelm, J. (2000). Expression, purification, and properties of Rab8 function in actin cortical skeleton organization and polarized transport. *Methods Enzymol.* **329**, 188-196.
Peränen, J., Auvinen, P., Virta, H., Wepf, R. and Simons, K. (1996). Rab8 promotes polarized membrane transport through reorganization of actin and microtubules in fibroblasts. *J. Cell Biol.* **135**, 153-167.
Powelka, A. M., Sun, J., Li, J., Gao, M., Shaw, L. M., Sonnenberg, A. and Hsu, V. W. (2004). Stimulation-dependent recycling of integrin beta1 regulated by Arf6 and Rab11. *Traffic* **5**, 20-36.
Powell, R. R. and Temesvari, L. A. (2004). Involvement of a Rab8-like protein of Dictyostelium discoideum, Sas1, in the formation of membrane extensions, secretion and adhesion during development. *Microbiology* **150**, 2513-2525.
Prignet, M., Dubois, T., Raposo, G., Derrien, V., Tenza, D., Rossé, C., Camonis, J. and Chavrier, P. (2003). Arf6 controls post-endocytic recycling through its downstream exocyst complex effector. *J. Cell Biol.* **163**, 1111-1121.
Radhakrishna, H. and Donaldson, J. G. (1997). ADP-ribosylation factor 6 regulates a novel plasma membrane recycling pathway. *J. Cell Biol.* **139**, 49-61.
Rezaie, T., Child, A., Hitchings, R., Brice, G., Miller, L., Coca-Prados, M., Heon, E., Krupin, T., Ritch, R., Kreutzer, D. et al. (2002). Adult-onset primary open-angle glaucoma caused by mutations in optineurin. *Science* **295**, 1077-1079.
Rodriguez, O. C. and Cheney, R. E. (2002). Human myosin-Vc is a novel class V myosin expressed in epithelial cells. *J. Cell Sci.* **115**, 991-1004.
Rodriguez-Gabin, A. G., Cammer, M., Amlazan, G., Charron, M. and Larocca, J. N. (2001). Role of rRab22b, an oligodendrocyte protein, in regulation of transport of vesicles from trans Golgi to endocytic compartments. *J. Neurosci. Res.* **66**, 1149-1160.
Sahlender, D. A., Roberts, R. C., Arden, S. D., Spudich, G., Taylor, M. J., Luzio, J. P., Kendrick-Jones, J. and Buss, F. (2005). Optineurin links myosin VI to the Golgi complex and is involved in Golgi organization and exocytosis. *J. Cell Biol.* **169**, 285-295.
Santy, L. C. (2002). Characterization of a fast-cycling ADP-ribosylation factor 6 mutant. *J. Biol. Chem.* **277**, 40185-40188.
Schlunck, G., Damke, H., Kiosses, W. B., Rusk, N., Symons, M. H., Waterman-Storer, C. M., Schmid, S. L. and Schwartz, M. A. (2004). Modulation of Rac localization and function by dynamin. *Mol. Biol. Cell* **15**, 256-267.
Schuck, S., Manninen, A., Honsho, M., Fullekrug, J. and Simons, K. (2004). Generation of single and double knockdowns in polarized epithelial cells by retrovirus-mediated RNA intereference. *Proc. Natl. Acad. Sci. USA* **101**, 4912-4917.
Shogomori, H. and Futerman, A. H. (2001). Cholera toxin is found in detergent-insoluble rafts/domains at the cell surface of hippocampal neurons but is internalized via a raft-independent mechanism. *J. Biol. Chem.* **276**, 9182-9188.
Ullrich, O., Reinsch, S., Urbé, S., Zerial, M. and Parton, R. (1996). Rab11 regulates recycling through the pericentriolar recycling endosome. *J. Cell Biol.* **135**, 913-924.
Vartiainen, M., Ojala, P. J., Auvinen, P., Peränen, J. and Lappalainen, P. (2000). Mouse A6/twinfilin is an actin monomer-binding protein that localizes to the regions of rapid actin dynamics. *Mol. Cell. Biol.* **20**, 1772-1783.
Zerial, M. and McBride, H. (2001). Rab proteins as membrane organizers. *Nat. Rev. Mol. Cell Biol.* **2**, 107-117.
Zhang, K.-Z., Westberg, J. A., Hölttä, E. and Andersson, L. C. (1996). BCL2 regulates neural differentiation. *Proc. Natl. Acad. Sci. USA* **93**, 4504-4508.

Journal of Cell Science